ARTICLE   OPEN

An effective method to screen sodium-based layered materials for sodium ion batteries

Xu Zhang[1], Zihe Zhang[1], Sai Yao[1], An Chen[1], Xudong Zhao[1] and Zhen Zhou [iD][1]

Due to the high cost and insufficient resource of lithium, sodium-ion batteries are widely investigated for large-scale applications. Typically, insertion-type materials possess better cyclic stability than alloy-type and conversion-type ones. Therefore, in this work, we proposed a facile and effective method to screen sodium-based layered materials based on Materials Project database as potential candidate insertion-type materials for sodium ion batteries. The obtained Na-based layered materials contains 38 kinds of space group, which reveals that the credibility of our screening approach would not be affected by the space group. Then, some important indexes of the representative materials, including the average voltage, volume change and sodium ion mobility, were further studied by means of density functional theory computations. Some materials with extremely low volume changes and Na diffusion barriers are promising candidates for sodium ion batteries. We believe that our classification algorithm could also be used to search for other alkali and multivalent ion-based layered materials, to accelerate the development of battery materials.

INTRODUCTION

Large-scale energy storage systems for the grid are extremely important for the storage and utilization of the renewable resources, such as solar and wind power.[1,2] Electrochemical energy storage could satisfy the demand of different grid functions.[3] Currently, lithium-ion batteries (LIBs) have become the most widely used devices for energy storage.[4,5] However, the high cost and insufficient resource of lithium inhibit the applications of LIBs in the large-scale electrochemical energy storage.[6] Sodium-ion batteries (SIBs) are extensively investigated as the most promising alternatives to LIBs due to the natural abundance and appropriate electrode potential.[1,7,8] However, the ionic radius of Na^+ is 55% larger than that of Li^+, requiring the host framework with larger space for the storage and transport of Na^+. Therefore, simply replacing the electrode materials for SIBs with those for LIBs is impracticable, which makes seeking for eligible Na^+ host materials extremely important.

Some typical insertion-type electrode materials, such as $Na_{0.44}MnO_2$, Na_xCoO_2,[9] $Na_{0.66}Co_{0.5}Mn_{0.5}O_2$,[10] $Li_4Ti_5O_{12}$,[11] and $Na_2Ti_3O_7$,[12] were widely investigated owing to their superior cyclic stability to the alloy-type and conversion-type ones.[13] Among them, Na-containing layered materials have attracted extensive attention since the layered structure ensures the reversible intercalation/de-intercalation of Na^+ without serious lattice changes, leading to good cyclic stability and excellent ionic conductivity. By means of density functional theory (DFT) computations, many previous reports proposed various electrode materials for LIBs, SIBs, and multivalent ion batteries, which greatly promoted their development.[14–17] Recently, with the fast development of high-performance computations, high-throughput computational materials design has attracted much attention and improved the efficiency of materials design, further accelerating the investigations on materials for various fields, especially LIBs.[18–22]

Therefore, in this work, more than 60,000 inorganic compounds in Materials Project (MP) Database[23,24] were investigated to search for sodium-based layered materials which can potentially be applied as insertion-type electrode materials for SIBs. Then by means of DFT computations, some important indexes of the representative materials, including the average voltage, volume change and sodium ion mobility, were examined. Besides Na-based layered materials, we believe that other alkali and multi-valent ion-based layered materials can also be searched by using this method, which might favor the development of electrode materials for batteries.

RESULTS AND DISCUSSION

Our screening approach for Na-based layered materials is shown in Fig. 1. After the materials screening, over 150 kinds of Na-based layered materials were obtained. The obtained Na-based layered materials contain 38 kinds of space group, as shown in Fig. 2, which belongs to six kinds of crystal systems except the cubic. The results indicate that the accuracy of our screening approach would not be affected by the space group of candidate materials.

The structures of some representative Na-based layered materials are shown in Fig. 3. Na atoms in these materials are mainly distributed between two layers, indicating that Na atoms could intercalate/de-intercalate with low energy barriers and therefore, these materials can be potentially used as insertion-type electrode materials for SIBs. The results further suggest that our screening approach is highly efficient and credible. This classification algorithm could also be employed to search for other alkali and multivalent ion-based layered materials as potential insertion-type electrode materials.

[1]School of Materials Science and Engineering, National Institute for Advanced Materials, Computational Centre for Molecular Science, Institute of New Energy Material Chemistry, Collaborative Innovation Center of Chemical Science and Engineering (Tianjin), Nankai University, Tianjin 300350, China
Correspondence: Zhen Zhou (zhouzhen@nankai.edu.cn)

npj

An effective method to screen sodium-based layered...
X Zhang et al.

2
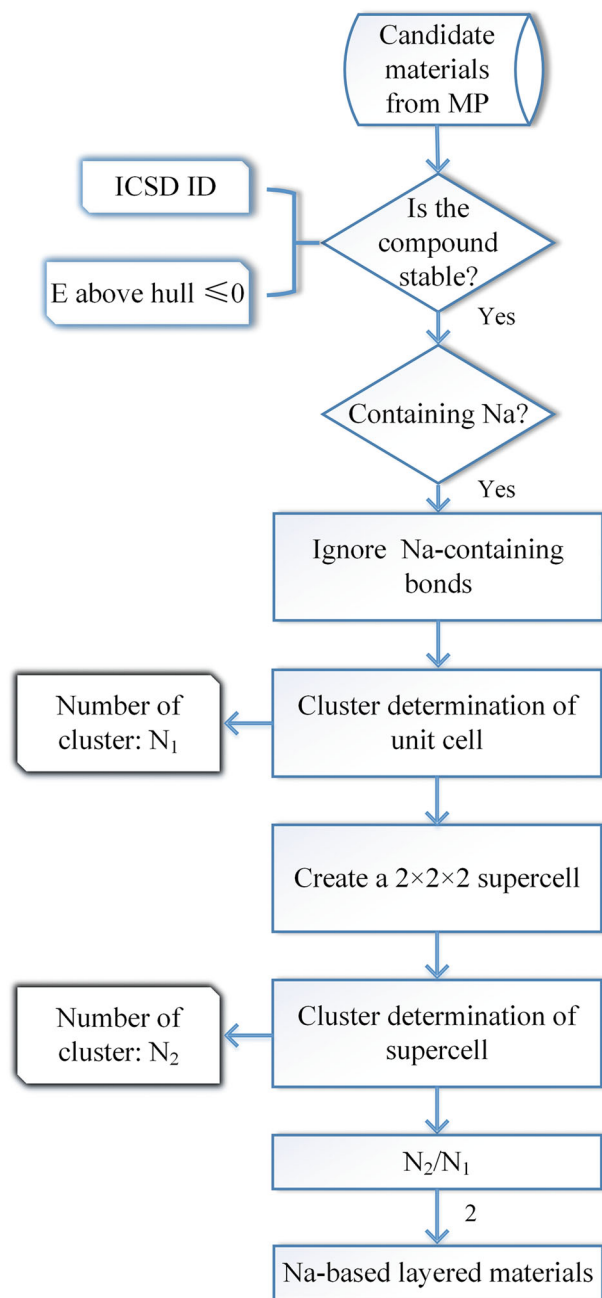
Fig. 1 Flow diagram of the screening approach for Na-based layered materials

To further verify the effectiveness of this method to explore electrode materials for SIBs, some important indexes of representative materials, including the average voltage, volume change and sodium ion mobility were further investigated. The geometries were firstly optimized and the lattice constants are shown in Supplementary Table 1, which are consistent with the experimental data. Some experimentally widely investigated layered materials for SIBs, such as Na-based layered transition metal oxides (TMOs), $NaMO_2$ ($M = Co$, Fe, V, Ni, etc),[13,25,26] were successfully achieved through screening. Na-based layered TM sulfides, $NaMS_2$ ($M = Ti$, Sc, Nb, etc), which have similar structures to TMOs, were also obtained, as well as layered TM fluorides, which could possess higher electrode potentials.

Then, the average intercalation voltages were computed based on the reaction energy of $Na_n + X \rightarrow Na_nX$, where n is the number of intercalating Na, and X is the rest of the compounds. The average intercalation voltage and volume change of the representative Na-based layered compounds are shown in Fig. 4 and Supplementary Table 2. The volume change is a critical parameter for electrode materials during Na intercalation/de-intercalation. Large volume changes could lead to the tremendous damage to electrodes, causing the loss of electrical contact and rapid capacity fading. Compared with alloy- and conversion-type electrode materials, the superior cyclic stability of insertion-type materials lies in much lower volume change during Na insertion/extraction. As shown in Fig. 4 and Supplementary Table 2, the volume changes of most materials are smaller than 25%, and for $NaTiF_4$ and $Na_2Cu(CO_3)_2$, minor volume changes of 13% imply good cyclic stability.

However, for some materials as shown in Supplementary Fig. 1, the volume change is higher than 50%. After Na^+ de-intercalation, the interlayer spacing decreases dramatically, causing large volume change and collapse of the layered structure. To settle the issue, some Na atoms should be kept in the materials to support the layered structure during the de-intercalation of Na. Besides, introducing heteroatom as pillars is another effective method to improve the structural stability.[27] The average intercalation voltages of many representative materials range from 2.5 to 4.5 V, which indicates that they have the potential to be used as cathode materials for SIBs.

The corresponding gravimetric capacity is also listed in Supplementary Table 2. It is important to note that the gravimetric capacity was computed based on the number of Na that the materials naturally possess. In experiments, some materials could accommodate extra Na atoms. For example, recently, $Na_2Mn_3O_7$ has been investigated as an electrode material for SIBs, and the results indicate that it could reversibly insert and extract two extra Na atoms.[28] $Na_2Ti_3O_7$, a widely investigated SIB electrode material, could also accommodate more Na atoms.[12]

Besides the materials that have been investigated for SIBs before, many materials are proposed as potential insertion-type electrode materials. Metal fluorides possess high average voltage and low volume change, especially $NaVF_4$ with an average voltage of 4.30 V, which would be promising candidates for cathode materials of SIBs. $Na_2Cu(CO_3)_2$, which has a low volume change of 13%, and a high average voltage of 4.39 V, can also be potentially applied as a cathode material. Some other materials, such as $Na_2Zr(CuS_2)_2$, $Na(CuO)_2$, and $Na_3Co_2SbO_6$, were also found with appropriate voltage and low volume change.

The rate performance of SIB electrode materials heavily depends on Na ion mobility; therefore, it is important to estimate the diffusion of Na in the interlayer. The climbing-image nudged elastic band (CI-NEB) method, which has been successfully applied in the study of ion diffusion,[17,29–31] was adopted to simulate the migration of Na. The energy profiles and barriers are shown in Fig. 5 and Table 1. Due to their special layered structure, the diffusion barriers of Na in the interlayer are quite low. The computed diffusion barrier of Na in $NaCoO_2$ is only 0.31 eV, which is consistent with those in previous reports.[32,33] For Na-based layered TM sulfides, the diffusion barriers are even lower (0.22 eV for $NaScS_2$ and 0.19 eV for $NaTiS_2$), which could be attributed to the lower electronegativity of S atoms. However, for some materials, such as NaAlSi, the diffusion barriers are higher than 0.6 eV, which can be ascribed to the large volume change.

Then, the electronic conductivity can be evaluated based on the band gaps obtained from MP database in Table 1 and the density of states in Supplementary Fig. 2. Among them, $Na_2Ti_3O_7$ possesses the largest band gap of 2.99 eV, which would cause rather low electronic conductivity. In experiments, some promising solutions could be applied to overcome this challenge, such as chemical modification and morphology control.[12,34,35] Besides, the band gaps of other materials are lower than that of $Na_2Ti_3O_7$, indicating better electronic conductivity. The partial density of

An effective method to screen sodium-based layered…
X Zhang et al.

npj

3
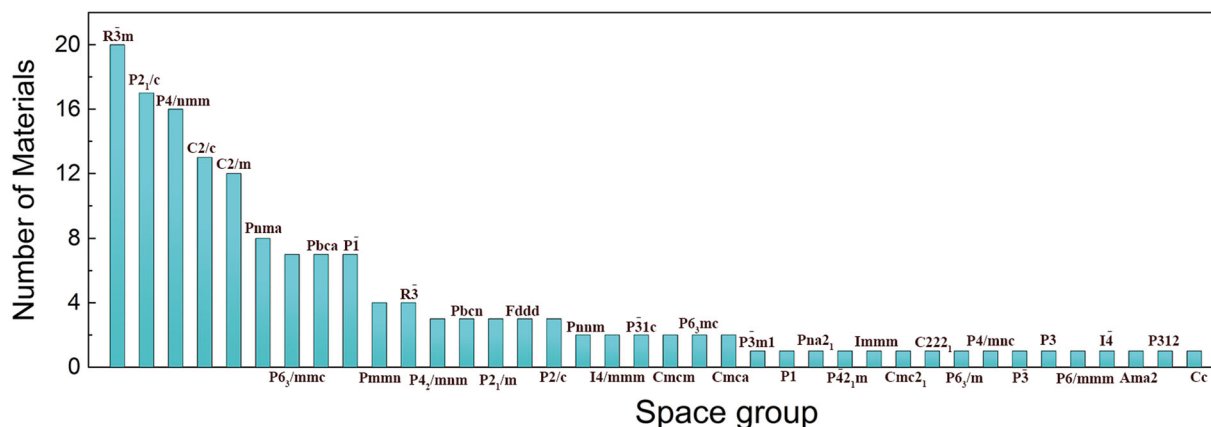
**Fig. 2** Distribution of space groups for the obtained Na-based layered materials
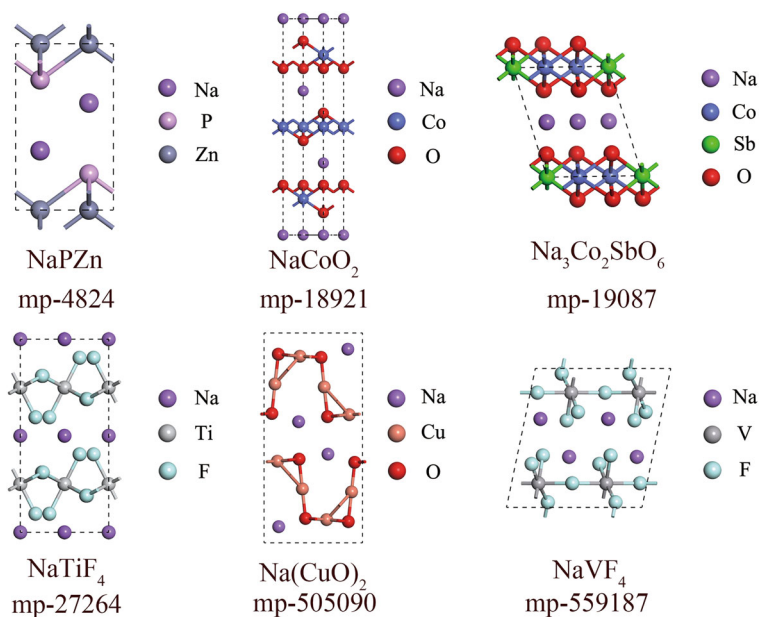
Fig. 3 Structures of some representative Na-based layered materials. The purple balls represent Na
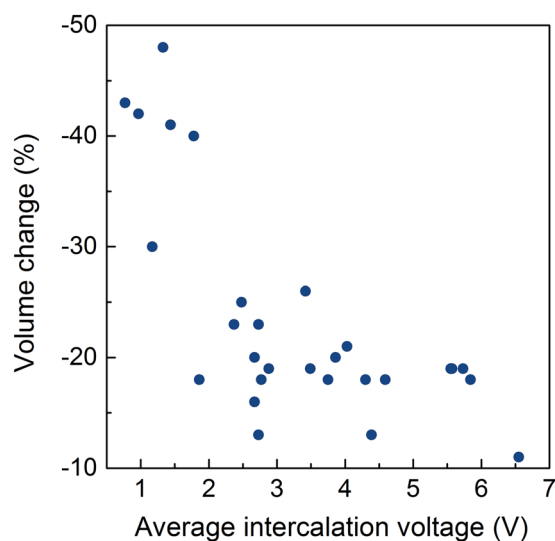
Fig. 4 The volume change after the de-intercalation of Na vs. average intercalation voltage

states (PDOS) reveals that Na contributes little to the states near the Fermi level. For some materials, such as $NaTiS_2$, the high peaks around the Fermi level imply high-concentration carriers and thus good electronic conductivity.

Based on the computed average voltage, volume change, gravimetric capacity, diffusion barrier and band gap, the electrochemical performance of representative Na-based layered materials for SIBs could be predicted. Compared with alloy-type and conversion-type materials, Na-based layered materials possess lower volume change after the de-intercalation of Na. The volume change of most materials is lower than 25%. Besides, the diffusion barrier of Na in the interlayer is extremely low, indicating excellent rate performance. In this work, we proposed some insertion-type electrode materials for SIBs, such as $Na(CuO)_2$, $NaTiF_4$, $Na_2Zr(CuS_2)_2$, $Na_3Co_2SbO_6$, and $Na_2Cu(CO_3)_2$, which possess appropriate voltage, high capacity, low volume change, Na diffusion barrier and band gap, and can be potentially used as cathode materials for SIBs. Detailed computations about the voltage and volume change for $Na_3Co_2SbO_6$ and $Na_2Cu(CO_3)_2$ are shown in Supplementary Fig. 3 and Supplementary Table 3. We would like to invite experimental colleagues to explore the practical performances of these materials in SIBs.

npj

An effective method to screen sodium-based layered...
X Zhang et al.

4
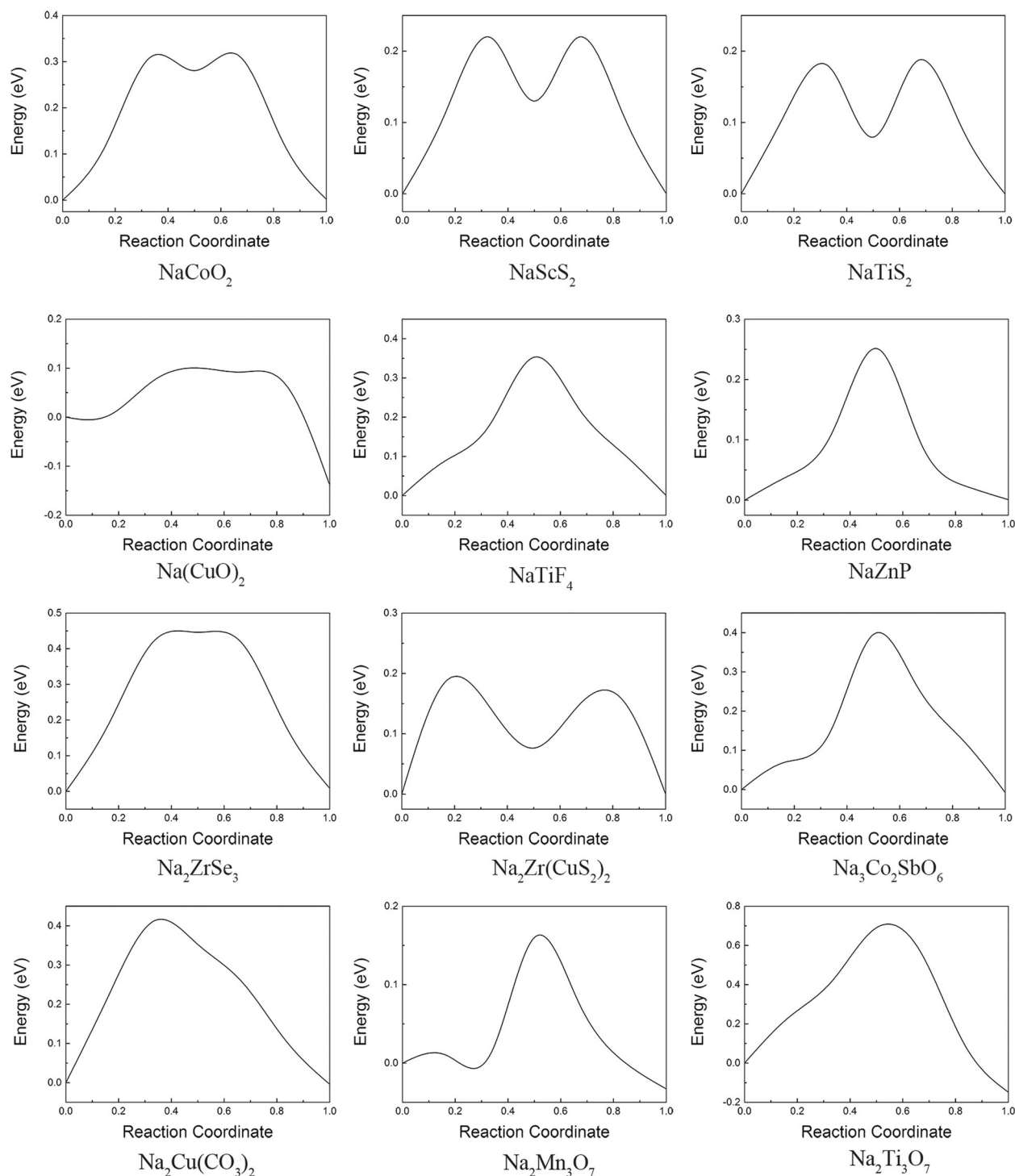
Fig. 5 Calculated minimum energy profiles of Na migration at the interlayer in some representative Na-based layered materials

In conclusion, we proposed a facile and effective method to search for sodium-based layered materials from MP database. The obtained layered materials contain 38 kinds of space group, indicating that our screening approach would not be affected by the space group. Then the average voltage, volume change and Na ion mobility were further investigated by means of DFT. The results confirm that the volume change and Na ion diffusion barrier are extremely low, making them promising candidate electrode materials for SIBs. We believe that our method could also be employed to search for other alkali and multivalent ion-based layered compounds as potential insertion-type electrode materials, and further accelerate the development of next-generation batteries.

METHODS

Vienna ab initio simulation package (VASP) was used to perform DFT computations.[36] The ion-electron interaction was described by using the

An effective method to screen sodium-based layered...
X Zhang et al.

np|

5

Table 1. The energy barrier (eV) of Na ion migration in the interlayer and the band gap (eV) for some representative Na-based layered materials

Formula	Energy barrier	Band gap
$NaCoO_2$	0.31	2.11
$NaScS_2$	0.22	1.81
$NaTiS_2$	0.19	0
$Na(CuO)_2$	0.10	0
$NaTiF_4$	0.35	0.20
$NaZnP$	0.25	0.91
$NaAlSi$	0.63	0
Na_2ZrSe_3	0.45	1.32
$Na_2Zr(CuS_2)_2$	0.19	0.01
$Na_3Co_2SbO_6$	0.40	1.91
$Na_2Cu(CO_3)_2$	0.41	0.49
$Na_2Mn_3O_7$	0.16	1.41
$Na_2Ti_3O_7$	0.69	2.99

projector augmented wave (PAW) method.[37] A 520 eV cutoff was applied for the plane-wave basis set. The functional of Perdew, Burke, and Ernzerhof (PBE) was employed to describe the exchange-correlation energy.[38] In order to accurately deal with the van der Waals force for weak interactions, the DFT-D3 method with Becke-Jonson damping was used.[39,40] K-point separation of 0.03 $Å^{-1}$ was employed. Considering the strong electron correlation effects, the U−J parameters were applied as the same as those adoped by Materials Project.[23] Also, magnetic ions were intialized ferromagnetically. The energy barriers of Na ion migration were computed by the CI-NEB method.[41] The average voltage was caculated as:

$$V_{ave} = (E_{de} + nE_{Na} - E_{int})/(ne) \quad (1)$$

where E_{de}, E_{int}, and E_{Na} represent the energy of the Na de-intercalation and intercalation structure, and the energy of Na atom in the metal crystal, respectively; n is the number of intercalated Na. The volume change was computed according to

$$v_{change} = (v_{de} - v_{in})/v_{in} \quad (2)$$

where v_{in} and v_{de} represent the volume before and after the de-intercalation of Na.

The inorganic materials from MP database are the candidates for screening. The stability of the candidate compound was examined by using two criteria, (i) the compound must have an Inorganic Crystal Structure Database (ICSD)[42] ID, indicating the experimental feasibility; (ii) the energy above convex hull must be zero, which ensures that it is the most energetically stable phase compared with its competing phases. Besides, only the compounds containing Na were chosen to ensure their capability for Na accommodation.

We proposed a simple method to search for Na-based layered materials. The covalent bonds in the unit cell of the candidate materials were identified based on:

$$T_1 \times \left(r_i^{cov} + r_j^{cov} \right) < d_{ij} < T_2 \times \left(r_i^{cov} + r_j^{cov} \right) \quad (3)$$

in which d_{ij} is the distance between the atom i and j; r_i^{cov} and r_j^{cov} are the experiential covalent radius of atom i and j, respectively; and T_1 and T_2 represent the lower and upper bond-length tolerance, respectively. In this work, T_1 and T_2 were set as 0.6 and 1.15, respectively, which were also applied as default values in Materials Studio. The Na-containing bonds in the candidate materials were ignored in order to make sure a precise evaluation of the structure of other atoms. Then, the atoms connected by covalent bonds were regarded as a cluster, and the number of clusters in a unit cell was defined as N_1. Similarly, the number of clusters in a $2 \times 2 \times 2$ supercell was denoted by N_2. If $N_2/N_1 = 2$, the compounds can be judged to be Na-based layered materials.

Data availability

The authors declare that the data supporting the findings of this study are available within the paper, and the comparison of the lattice parameters,

average intercalation voltage, volume change, gravimetric capacity, atomic structure and density of states for some representative Na-based layered materials and the average voltage profile and volume change of $Na_2Cu(CO_3)_2$ and $Na_3Co_2SbO_6$ are available in its supplementary information files.

AUTHOR CONTRIBUTIONS

X.Z. performed the computations, analyzed the results and wrote the manuscript. Z.H. Z., S.Y., and A.C. advised on computations. X.Z., Z.H.Z., and X.D.Z. proposed and edited the screening algorithm. Z.Z. analyzed the results and supervised the project. All authors reviewed and approved the manuscript.

ADDITIONAL INFORMATION

Supplementary information accompanies the paper on the *npj Computational Materials* website (https://doi.org/10.1038/s41524-018-0070-2).

REFERENCES

1. Yabuuchi, N., Kubota, K., Dahbi, M. & Komaba, S. Research development on sodium-ion batteries. *Chem. Rev.* **114**, 11636–11682 (2014).
2. Yang, J., Zhou, X., Wu, D., Zhao, X. & Zhou, Z. S-doped N-rich carbon nanosheets with expanded interlayer distance as anode materials for sodium-ion batteries. *Adv. Mater.* **29**, 1604108 (2017).
3. Dunn, B., Kamath, H. & Tarascon, J.-M. Electrical energy storage for the grid: a battery of choices. *Science* **334**, 928–935 (2011).
4. Tarascon, J.-M. & Armand, M. Issues and challenges facing rechargeable lithium batteries. *Nature* **414**, 359–367 (2001).
5. Zhong, Y. et al. Orderly packed anodes for high-power lithium-ion batteries with super-long cycle life: rational design of $MnCO_3$/large-area graphene composites. *Adv. Mater.* **27**, 806–812 (2015).
6. Tarascon, J. M. Is lithium the new gold? *Nat. Chem.* **2**, 510 (2010).
7. Zhu, Y.-E. et al. Fast sodium storage in TiO_2@CNT@C nanorods for high-performance Na-ion capacitors. *Adv. Energy Mater.* 1701222 (2017).
8. Yang, L. et al. $T-Nb_2O_5$/C nanofibers prepared through electrospinning with prolonged cycle durability for high-rate sodium-ion batteries induced by pseudocapacitance. *Small* 1702588 (2017).
9. Palomares, V. et al. Na-ion batteries, recent advances and present challenges to become low cost energy storage systems. *Energy Environ. Sci.* **5**, 5884–5901 (2012).
10. Zhu, Y.-E. et al. A P2-$Na_{0.67}Co_{0.5}Mn_{0.5}O_2$cathode material with excellent rate capability and cycling stability for sodium ion batteries. *J. Mater. Chem. A* **4**, 11103–11109 (2016).
11. Zhou, Q. et al. Synthesis of lithium titanate nanorods as anode materials for lithium and sodium ion batteries with superior electrochemical performance. *J. Power Sources* **283**, 243–250 (2015).
12. Pan, H. et al. Sodium storage and transport properties in layered $Na_2Ti_3O_7$ for room-temperature sodium-ion batteries. *Adv. Energy Mater.* **3**, 1186–1194 (2013).
13. Li, F. & Zhou, Z. Micro/nanostructured materials for sodium ion batteries and capacitors. *Small* **14**, 1702961 (2018).
14. Urban, A., Seo, D.-H. & Ceder, G. Computational understanding of Li-ion batteries. *npj Comput. Mater.* **2**, 16002 (2016).
15. Islam, M. S. & Fisher, C. A. Lithium and sodium battery cathode materials: computational insights into voltage, diffusion and nanostructural properties. *Chem. Soc. Rev.* **43**, 185–204 (2014).
16. Bhatt, M. D. & O'Dwyer, C. Recent progress in theoretical and computational investigations of Li-ion battery materials and electrolytes. *Phys. Chem. Chem. Phys.* **17**, 4799–4844 (2015).
17. Tang, Q., Zhou, Z. & Shen, P. Are MXenes promising anode materials for Li ion batteries? computational studies on electronic properties and Li storage capability of Ti_3C_2 and $Ti_3C_2X_2$ (X=F, OH) monolayer. *J. Am. Chem. Soc.* **134**, 16909–16916 (2012).

np
An effective method to screen sodium-based layered...
X Zhang et al.

6

18. Hautier, G. et al. Phosphates as lithium-ion battery cathodes: an evaluation based on high-throughput ab initio calculations. *Chem. Mater.* **23**, 3495–3508 (2011).

19. Kirklin, S., Meredig, B. & Wolverton, C. High-throughput computational screening of new Li-ion battery anode materials. *Adv. Energy Mater.* **3**, 252–262 (2013).

20. Jain, A., Hautier, G., Ong, S. P., Dacek, S. & Ceder, G. Relating voltage and thermal safety in Li-ion battery cathodes: A high-throughput computational study. *Phys. Chem. Chem. Phys.* **17**, 5942–5953 (2015).

21. Aykol, M. et al. High-throughput computational design of cathode coatings for Li-ion batteries. *Nat. Commun.* **7**, 13779 (2016).

22. Sendek, A. D. et al. Holistic computational structure screening of more than 12000 candidates for solid lithium-ion conductor materials. *Energy Environ. Sci.* **10**, 306–320 (2017).

23. Jain, A. et al. Commentary: the materials project: a materials genome approach to accelerating materials innovation. *APL Mat.* **1**, 011002 (2013).

24. Ong, S. P. et al. The Materials Application ProgrammingInterface (API): A simple, flexible and efficient API for materials data based on REpresentational State Transfer (REST) principles. *Comp. Mater. Sci.* **97**, 209–215 (2015).

25. Fang, C. et al. Routes to high energy cathodes of sodium-ion batteries. *Adv. Energy Mater.* **6**, 1501727 (2016).

26. Hwang, J. Y., Myung, S. T. & Sun, Y. K. Sodium-ion batteries: present and future. *Chem. Soc. Rev.* **46**, 3529–3614 (2017).

27. Liang, J. et al. Could Li/Ni disorder be utilized positively? Combined experimental and computational investigation on pillar effect of Ni at Li sites on $LiCoO_2$ at high voltages. *Electrochim. Acta* **146**, 784–791 (2014).

28. Adamczyk, E. & Pralong, V. $Na_2Mn_3O_7$: a suitable electrode material for Na-ion batteries? *Chem. Mater.* **29**, 4645–4648 (2017).

29. Zhao, X. et al Ab-initio investigations on bulk and monolayer V_2O_5 as cathode materials for Li-, Na-, K- and Mg-Ion batteries. *J. Mater. Chem. A* **4**, 16606–16611 (2016).

30. Zhang, X. et al. Tetragonal-structured anisotropic 2D metal nitride monolayers and their halides with versatile promises in energy storage and conversion. *J. Mater. Chem. A* **5**, 2870–2875 (2017).

31. Liu, M. et al. Spinel compounds as multivalent battery cathodes: a systematic evaluation based on ab initio calculations. *Energy Environ. Sci.* **8**, 964–974 (2015).

32. Li, G., Yue, X., Luo, G. & Zhao, J. Electrode potential and activation energy of sodium transition-metal oxides as cathode materials for sodium batteries: a first-principles investigation. *Comp. Mater. Sci.* **106**, 15–22 (2015).

33. Su, J., Pei, Y., Yang, Z. & Wang, X. First-principles investigation on the structural, electronic properties and diffusion barriers of Mg/Al doped $NaCoO_2$ as the cathode material of rechargeable sodium batteries. *RSC Adv.* **5**, 27229–27234 (2015).

34. Fu, S., Ni, J., Xu, Y., Zhang, Q. & Li, L. Hydrogenation driven conductive $Na_2Ti_3O_7$ nanoarrays as robust binder-free anodes for sodium-ion batteries. *Nano. Lett.* **16**, 4544–4551 (2016).

35. Ni, J. et al. Superior sodium storage in $Na_2Ti_3O_7$ nanotube arrays through surface engineering. *Adv. Energy Mater.* **6**, 1502568 (2016).

36. Kresse, G. & Furthmüller, J. Efficient iterative schemes for ab initio total-energy calculations using a plane-wave basis set. *Phys. Rev. B* **54**, 11169–11186 (1996).

37. Blöchl, P. E. Projector augmented-wave method. *Phys. Rev. B* **50**, 17953–17979 (1994).

38. Perdew, J. P., Burke, K. & Ernzerhof, M. Generalized gradient approximation made simple. *Phys. Rev. Lett.* **77**, 3865–3868 (1996).

39. Grimme, S., Antony, J., Ehrlich, S. & Krieg, H. A consistent and accurate ab initio parametrization of density functional dispersion correction (DFT-D) for the 94 elements H-Pu. *J. Chem. Phys.* **132**, 154104 (2010).

40. Grimme, S., Ehrlich, S. & Goerigk, L. Effect of the damping function in dispersion corrected density functional theory. *J. Comput. Chem.* **32**, 1456–1465 (2011).

41. Henkelman, G. & Jónsson, H. Improved tangent estimate in the nudged elastic band method for finding minimum energy paths and saddle points. *J. Chem. Phys.* **113**, 9978–9985 (2000).

42. Belsky, A., Hellenbrandt, M., Karen, V. L. & Luksch, P. New developments in the Inorganic Crystal Structure Database (ICSD): accessibility in support of materials research and design. *Acta Crytallogr. Sect. B* **58**, 364–369 (2002).